JOURNAL OF VIROLOGY, Oct. 1997, p. 7567–7578 Vol. 71, No. 10
0022-538X/97/$04.00+0

A Bulged Stem-Loop Structure in the 3′ Untranslated Region of the Genome of the Coronavirus Mouse Hepatitis Virus Is Essential for Replication

BILAN HSUE[1] AND PAUL S. MASTERS[1,2]*

Department of Biomedical Sciences, University at Albany, State University of New York,[1] and Wadsworth Center for Laboratories and Research, New York State Department of Health,[2] Albany, New York 12201

Received 7 April 1997/Accepted 10 July 1997

The 3′ untranslated region (UTR) of the positive-sense RNA genome of the coronavirus mouse hepatitis virus (MHV) contains sequences that are necessary for the synthesis of negative-strand viral RNA as well as sequences that may be crucial for both genomic and subgenomic positive-strand RNA synthesis. We have found that the entire 3′ UTR of MHV could be replaced by the 3′ UTR of bovine coronavirus (BCV), which diverges overall by 31% in nucleotide sequence. This exchange between two viruses that are separated by a species barrier was carried out by targeted RNA recombination. Our results define regions of the two 3′ UTRs that are functionally equivalent despite having substantial sequence substitutions, deletions, or insertions with respect to each other. More significantly, our attempts to generate an unallowed substitution of a particular portion of the BCV 3′ UTR for the corresponding region of the MHV 3′ UTR led to the discovery of a bulged stem-loop RNA secondary structure, adjacent to the stop codon of the nucleocapsid gene, that is essential for MHV viral RNA replication.

Coronaviruses are a family of single-stranded, positive-polarity RNA viruses having genomes of 26 to 31 kb that are the largest known replicating RNA molecules (36). Upon infection, coronavirus genomic RNA serves as the message for translation of a viral RNA-dependent RNA polymerase, which then copies the viral genome into a full-length negative-strand RNA. Presumably, the negative-strand RNA subsequently acts as a template for positive-strand RNA synthesis. In the life cycle of mouse hepatitis virus (MHV), a prototype coronavirus, six to seven 3′-coterminal subgenomic RNA species are synthesized in addition to the full-length genome (16, 42). All subgenomic RNAs contain a common 5′ leader sequence identical to the 5′ end of the viral genome. In MHV, this leader is approximately 70 nucleotides (nt) in length. In addition, each subgenomic RNA has a negative-strand RNA counterpart containing an antileader sequence at its very 3′ end (8, 32–34). The function of these subgenomic negative-strand species has not been clearly elucidated yet. Coronavirus RNA synthesis also involves a high frequency of homologous recombination, which has been hypothesized to occur by means of a template-switching mechanism (17).

Our understanding of coronavirus replication has been limited by the large size of the genome, which has been an obstacle to construction of a full-length cDNA clone for synthesis of infectious RNA. In this regard, a major breakthrough was the discovery of defective interfering (DI) RNAs of MHV (22, 23, 40) and, subsequently, of bovine coronavirus (BCV) (1), infectious bronchitis virus (29), and transmissible gastroenteritis coronavirus (25). DI RNAs are deletion mutants, usually far smaller than the genome, that replicate by capture of components of the viral RNA synthesis machinery, often interfering with the replication of viral genomic RNA. Thus, DI RNAs must carry the key sequence elements required for replication with the help of standard virus. Studies of naturally occurring and artificially constructed DI RNAs have shown that both 5′- and 3′-terminal portions of the MHV genome are required to make them functional.

The 5′ *cis*-acting elements essential for MHV DI RNA replication have been mapped by several groups. Deletion analysis of DIssE, a naturally occurring DI RNA of MHV strain JHM, has indicated that the 5′ 474 nt are sufficient for replication, and at least 446 nt are required (12). Consistent with this result are studies of MHV A59 DI RNAs, pB36 and deletion mutants of MIDI (21, 24). The constructed DI RNA pB36, patterned after a natural BCV DI RNA (1), comprises 467 nt from the 5′ end and 1,666 nt from the 3′ end of the genome. The study of deletion mutants of MIDI, which was derived from a naturally occurring DI RNA (40), showed that the minimal requirement of 5′ sequence was the first 466 nt (21). In apparent conflict with these findings, no 5′ segment of another MHV JHM DI RNA, DIssF, smaller than 859 nt was able to sustain replication (18). Another conflict in the mapping of *cis*-acting elements has arisen over the status of an internal sequence element located between nt 3113 and 3247 from the 5′ end of the genome. This has been shown to be required for replication of MHV JHM-derived DI RNAs (12, 18), but it is not necessary for the replication of MHV A59-derived DI RNAs (21, 24).

At the 3′ end of the genome, excluding the poly(A) tail, the minimal stretch of sequence required for replication of the MHV JHM DI RNA DIssE has been shown to be 417 to 463 nt (12); the corresponding value mapped for DIssF is 378 to 436 nt (18). In accord with this, deletion mapping of the MHV A59 DI RNA MIDI showed that the shortest length at the 3′ end that can support replication is 461 nt (41). Interestingly, the minimal *cis*-acting signal essential for negative-strand RNA synthesis is contained within only the last 55 nt at the 3′ terminus of the genome plus an undetermined amount of poly(A) tail (19). This implies that the *cis*-acting signals embedded upstream of nt 55 are required for positive-strand RNA synthesis, which has led to the suggestion that positive-

* Corresponding author. Mailing address: David Axelrod Institute, Wadsworth Center, NYSDOH, New Scotland Ave., P.O. Box 22002, Albany, NY 12201-2002. Phone: (518) 474-1283. Fax: (518) 473-1326.

TABLE 1. Plasmids constructed for this study

Plasmid	Nucleotide coordinates of MHV 3′ UTR replaced by BCV 3′ UTR[a]	Other modification(s)[b]
pBL10	1–266	8-nt insertion between nt 266 and 267
pBL34	1–266	8-nt insertion between nt 266 and 267
pBL50	18–266	BCV 3′ UTR inserted in reverse orientation
pBL31	None	nt 405–1365 of the MHV A59 N gene and nt 72–301 of 3′ UTR replaced by the corresponding regions of the MHV-1 N gene and 3′ UTR
pBL46	26–212	Point mutations A69T, G166A, A191T, and G279A in 3′ UTR
pBL47	26–212	Point mutations A84T, T141C, and T171C in 3′ UTR, and C1261T and A1358G in the N gene
pBL64	26–266	8-nt insertion between nt 266 and 267
pBL63	1–212	Point mutations A69T, G166A, A191T, and G279A in 3′ UTR
pBL82	1–300	Point mutation G267C and 8-nt insertion between nt 266 and 267
pBL75	1–233	8-nt insertion between nt 266 and 267
pBL69	1–263	
pBL77	1–300	Point mutation G267C
pBL79	1–233, 271–300	
pBL72	1–233	

[a] All coordinates are given according to the MHV sequence, numbered in the 3′-to-5′ direction from the end of the genome, as in Fig. 4.
[b] With the exception of pBL10 and pBL31, all plasmids also contain the BCV spacer B marker in the N gene.

strand RNA synthesis may require an interaction between the 5′ and 3′ termini of the viral genome (19).

Although the information derived from DI RNAs has provided insights into what RNA elements are required for MHV replication, some of it is contradictory and may not completely reflect the requirements for MHV genomic RNA synthesis. At the outset of this study, we sought to complement the DI RNA deletion analyses of other groups with a phylogenetic approach to examine the sequences or structures of the 3′ untranslated region (UTR) within the full genome required for viral replication. Since we have previously shown that it is possible to incorporate mutations into the nucleocapsid (N) gene and the 3′ UTR of MHV by targeted recombination (5, 15, 24, 27, 28), we sought to replace the MHV 3′ UTR with a similar sequence by this technique with the aim of revealing critical regions with respect to the MHV replication mechanism. Although the 3′ UTRs of different MHV strains are more than 99% conserved, which could be taken to reflect stringent RNA sequence or structure requirements, we set out to examine the possibility of replacing the MHV 3′ UTR with the corresponding region of the BCV genome, which has 69% sequence homology to its MHV counterpart. We have previously demonstrated that extensive exchanges between parts of the BCV and MHV N genes can be tolerated (28), and this led us to speculate that the replacement of the 3′ UTR between these two viral species might be feasible.

In this report, we describe how we incorporated the BCV 3′ UTR into the genome of MHV and, consequently, discovered a functionally essential RNA secondary structure immediately following the stop codon of the nucleocapsid gene.

MATERIALS AND METHODS

Virus and cells. All stocks of MHV wild-type, mutant, and recombinant viruses were grown in mouse 17Cl1 cells. Plaque titrations and plaque purifications were carried out with mouse L2 cells. Spinner cultures of L2 cells were maintained for synthetic RNA transfection by electroporation, as described previously (24).

Plasmid constructs. The parent for all plasmids constructed for this work was pB36, which is a T7 transcription vector encoding an MHV A59 DI RNA consisting of 467 nt of the 5′ end of the genome connected in frame, via a 48-nt linker, to the entire N gene and 3′ UTR, followed by a poly(A) tail of approximately 115 residues (24). Most chimeric BCV-MHV 3′ UTR constructs (Table 1) were generated by substitutions in the MHV 3′ UTR of the homologous regions of the BCV 3′ UTR taken from the BCV clone pLN (9) (or a pLN-derived chimeric construct), according to the sequence alignment shown in Fig. 4. Junctions between the MHV and BCV 3′ UTRs were created within regions of identity between the two sequences. The plasmids listed were constructed via two- or three-way ligations of fragments of other plasmids in Table 1 or, in some cases, via the generation of intermediary constructs not discussed here.

Within the vectors listed in Table 1, the only nonhomologous junction occurred in the initial construct, pBL10 (Fig. 1), and its descendants, in which a small 5′ segment of the MHV 3′ UTR terminated by a blunted *Bst*EII site was joined to a blunted *Dra*III-*Msc*I fragment containing most of the BCV 3′ UTR. This junction resulted in an 8-nt insertion (5′GTGGTAAG3′) between nt 266 and 267. [The coordinate system used for the 3′ UTR throughout this paper is according to the MHV sequence, beginning at the nucleotide adjacent to the poly(A) tail and ending at the nucleotide following the N gene stop codon.] With the exception of pBL10, all BCV-MHV chimeric constructs also contained a substitution at nt 1145 to 1191 of the MHV N gene, replacing the *Bst*XI-*Acc*I fragment with sequence encoding a phenotypically silent exchange of BCV residues in a portion of the spacer B region of the N protein (28). This spacer B marker was inserted into pBL10 with an oligonucleotide cassette, as described previously for pCK120 (28), to generate pBL34 (Fig. 1), and all subsequent constructs obtained this marker either from pBL34 or from pCK120.

Plasmids pBL46 and pBL47 (see Fig. 5A) were generated by the transfer of the *Acc*I (spacer B)-*Msc*I fragments of the PCR clones pBLTA148 and pBLTA128, respectively, into pBL34. pBL34 nt 22 and 25 were changed to their MHV counterparts and those of pBL46 were changed to their BCV counterparts by PCR mutagenesis and reinsertion of the *Ase*I-*Msc*I fragment of the 3′ UTR of each, giving rise to pBL64 and pBL63, respectively.

Plasmids pBL82, pBL75, pBL69, pBL77, pBL79, and pBL72 (see Fig. 7A), containing different combinations of the left and right arms of the putative bulged stem-loop structure, were constructed by the reassortment of PCR-generated fragments or fragments of previously constructed vectors. In each case, the fragment containing the left arm of the structure was bounded by the *Bst*EII (or blunted *Bst*EII) site in the loop and an upstream site in the N gene (either *Spe*I, *Nhe*I, or *Acc*I). The fragment containing the right arm of the structure was bounded by the *Bst*EII (or blunted *Dra*III) site in the loop and the downstream *Msc*I site in the 3′ UTR or the *Hin*dIII site following the poly(A) tract.

The only plasmid in Table 1 not containing BCV sequences was pBL31 (Fig. 2). This was constructed by substitution of the *Apa*I-*Sac*I fragment of the MHV A59 N gene and 3′ UTR in pB36 with the corresponding region of MHV-1 sequence from pMP101 (26) via a three-way ligation.

DNA manipulations were performed by standard methods (30). All ligation junctions and sequences of inserts generated by PCR were confirmed by dideoxy sequencing by the method of Sanger et al. (31) with a modified T7 DNA polymerase kit (Sequenase; U.S. Biochemical).

Targeted recombination. Mutations created in synthetic donor RNAs were incorporated into the 3′ UTR or the N gene of the MHV genome by targeted recombination with the thermolabile N gene deletion mutant Alb4 as the recipient virus (15, 24). Capped donor RNAs were synthesized from *Nsi*I- or *Hin*dIII-truncated vectors with a T7 polymerase transcription kit (Ambion) per the manufacturer's instructions, and one-half of each reaction mixture (estimated to contain 10 μg of RNA) was used directly for electroporation into Alb4-infected spinner culture L2 cells, under conditions described previously (24). Progeny-released viruses were subsequently subjected to plaque assay at 39°C with or without prior thermal inactivation, which was performed at 40°C and pH 6.5 for 24 h (15). Candidate recombinant viruses, selected as those forming

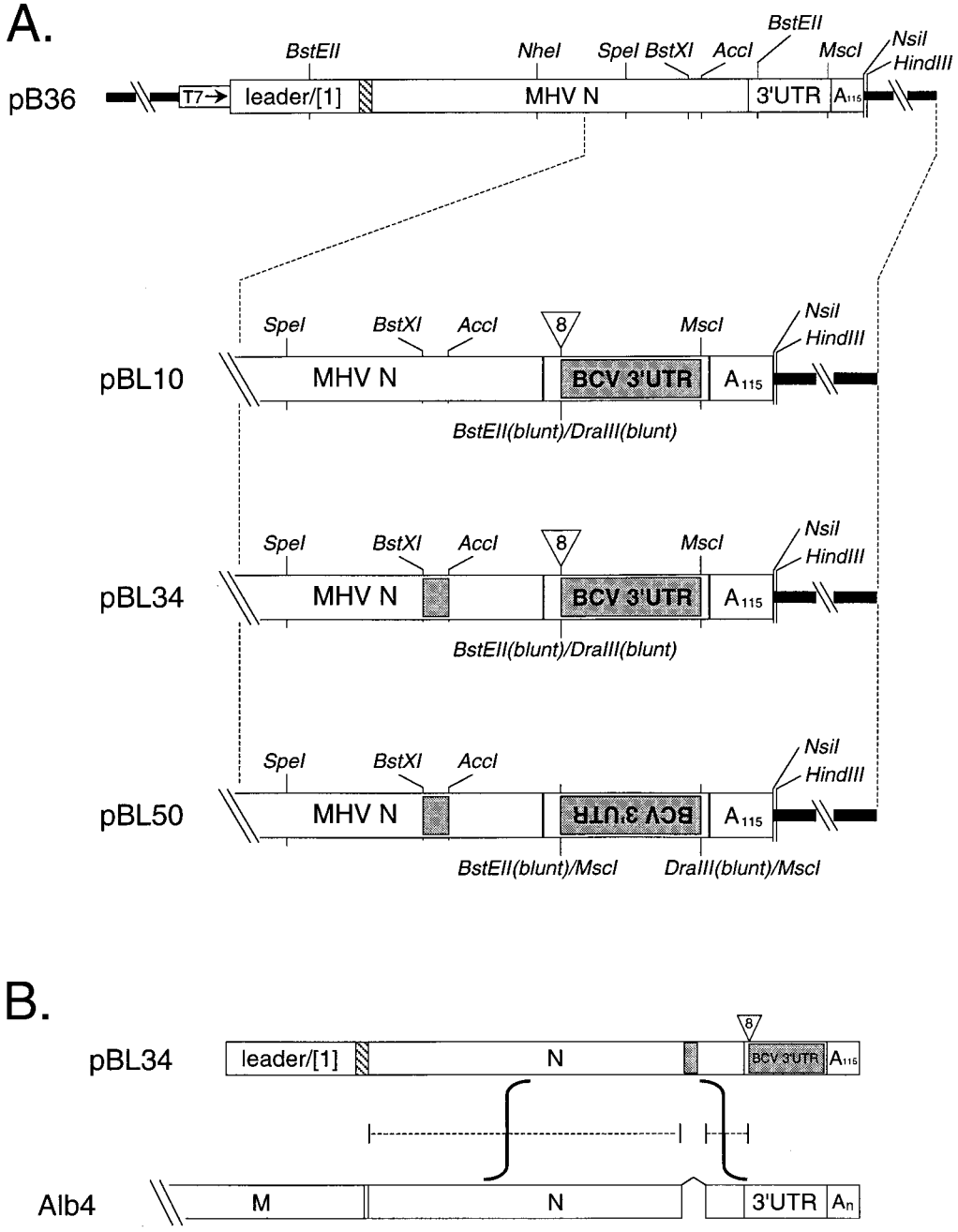

FIG. 1. Construction of transcription vectors for the synthesis of MHV DI RNAs containing almost the entire BCV 3′ UTR. (A) The parent plasmid, pB36, which has been described previously (24), encodes a DI RNA composed entirely of MHV components, except for a 48-nt linker region (hatched rectangle). Plasmid pBL10 contains all of the BCV 3′ UTR in place of the MHV 3′ UTR, except for the 35 nt immediately following the N gene stop codon; an 8-nt insertion created at the nonhomologous (blunted *Bst*EII-blunted *Dra*III) junction is indicated by a triangle. Plasmid pBL34 is identical to pBL10, except for the substitution of a portion of the spacer B region of the N gene as a marker. Plasmid pBL50 is identical to pBL34, except that the BCV 3′ UTR substitution is inserted in the opposite orientation. (B) Two crossover events and the limits between which they could occur proposed to give rise to recombinants obtained from pBL34 RNA and Alb4 recipient virus.

wild-type-size plaques at the nonpermissive temperature for Alb4, underwent plaque purification before further analysis.

Preparation and analysis of viral RNAs. Viral genomic RNA was isolated from virus purified by two cycles of equilibrium centrifugation on potassium tartrate-glycerol gradients as described in detail previously (5). Total cytoplasmic RNA derived from virus-infected 17Cl1 cell monolayers was purified either by a Nonidet P-40-gentle lysis method (14) or with Ultraspec reagent (Biotecx). RNA sequencing was carried out by a modified dideoxy chain termination procedure with avian myeloblastosis virus reverse transcriptase (Life Sciences) (4, 27).

Radiolabeling of viral RNA. The metabolic labeling of virus-specific RNA was performed essentially as reported previously (24). Briefly, spinner culture L2 cells were infected in suspension with wild-type MHV at a multiplicity of 1 to 5 PFU per cell. At 2 h postinfection, cells were electroporated with DI RNA as in targeted recombination experiments and plated onto a 20-cm^2 monolayer of 17Cl1 cells, and incubation was continued at 37°C until the monolayer contained roughly 50% syncytia (13 to 14 h). Cells were then labeled for 2 h with either [5,6-^{3}H]uridine or $^{32}P_i$ in Eagle's minimal essential medium containing 5% dialyzed fetal bovine serum and 20 μg of actinomycin D (Sigma) per ml. When $^{32}P_i$ was used, the labeling period was preceded by 2 h of starvation in medium containing 1/10 of the normal phosphate concentration, and the labeling medium was phosphate free. Total cytoplasmic RNA was purified, and samples containing equal amounts of radioactivity were analyzed by electrophoresis.

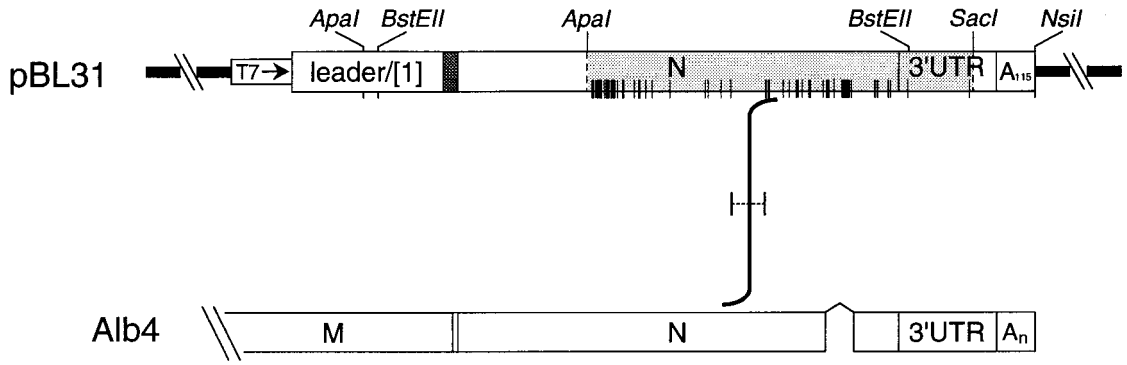

FIG. 2. Targeted RNA recombination between a donor RNA tagged at multiple sites and Alb4 recipient virus. Plasmid pBL31 contains portions of the MHV-1 N gene and 3′ UTR (shaded) in place of their MHV A59 counterparts, as detailed in Materials and Methods. Tick marks denote MHV-1 nucleotides that are different from those of MHV A59. The bracketed dotted line in the center of the figure marks the limits of the single crossover event observed for three independent recombinants analyzed in detail.

Recombinational PCR mutagenesis. The DNA shuffling technique devised by Stemmer (37, 38) was used to mutagenize pBL34 (Fig. 3B) in order to obtain derivative DI RNAs capable of replication. In brief, 7 μg of the *Spe*I-*Msc*I fragment of pBL34 (725 bp) was partially digested with 0.8 U of DNase I (RQ1; Promega) in 100 μl of 50 mM Tris-HCl (pH 8.0)–1 mM $MgCl_2$ for 20 min at room temperature. Fragment sizes ranging from 10 to 50 bp were recovered from a 2.5% agarose gel by electrophoresis onto a DE81 filter (Whatman), and DNA was eluted with 20 mM Tris-HCl (pH 8.0)–0.1 mM EDTA containing 1 M NaCl and then precipitated with ethanol. The recovered fragments were reassembled by primerless PCR with 2.5 U of *Taq* polymerase per 100 μl of reaction mixture as described previously (15). Reactions were run for 40 cycles of 1 min at 94°C, 1 min at 50°C, and 2 min at 72°C. A portion (2.5 μl) of the resulting heteroge-

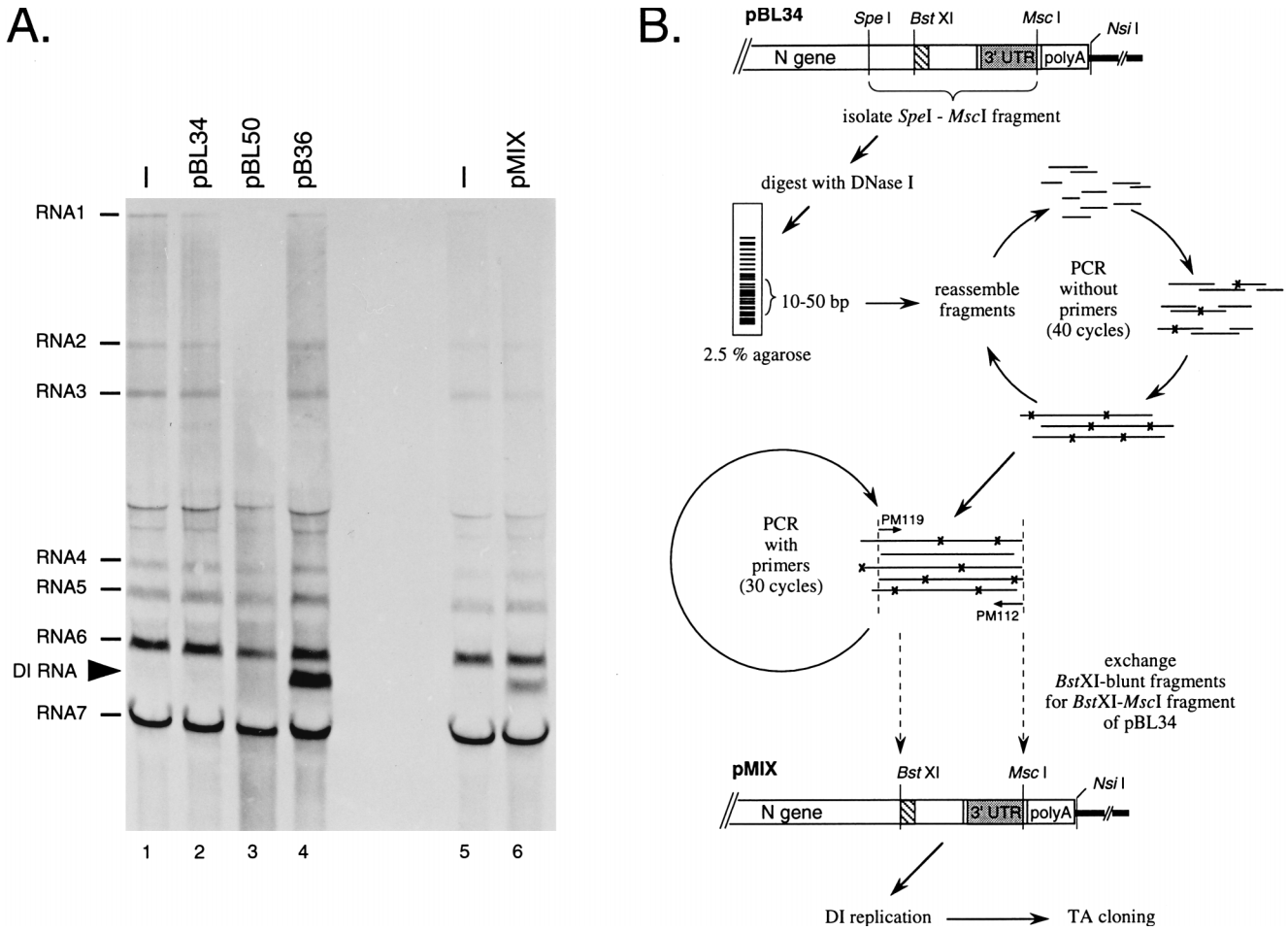

FIG. 3. Replicative ability of MHV and MHV-BCV chimeric DI RNAs. (A) Wild-type MHV-infected cells were transfected with the indicated DI RNA (lanes 2 to 4 and 6) or with H_2O (lanes 1 and 5) and then were labeled with 50 μCi of [5,6-^{3}H]uridine per ml. Purified cytoplasmic RNA was denatured with glyoxal and dimethyl sulfoxide, separated by electrophoresis through 1% agarose (30), and visualized by fluorography. (B) Strategy for recombinational PCR mutagenesis of the distal portion of pBL34 by the method of Stemmer (37, 38). Details are given in Materials and Methods.

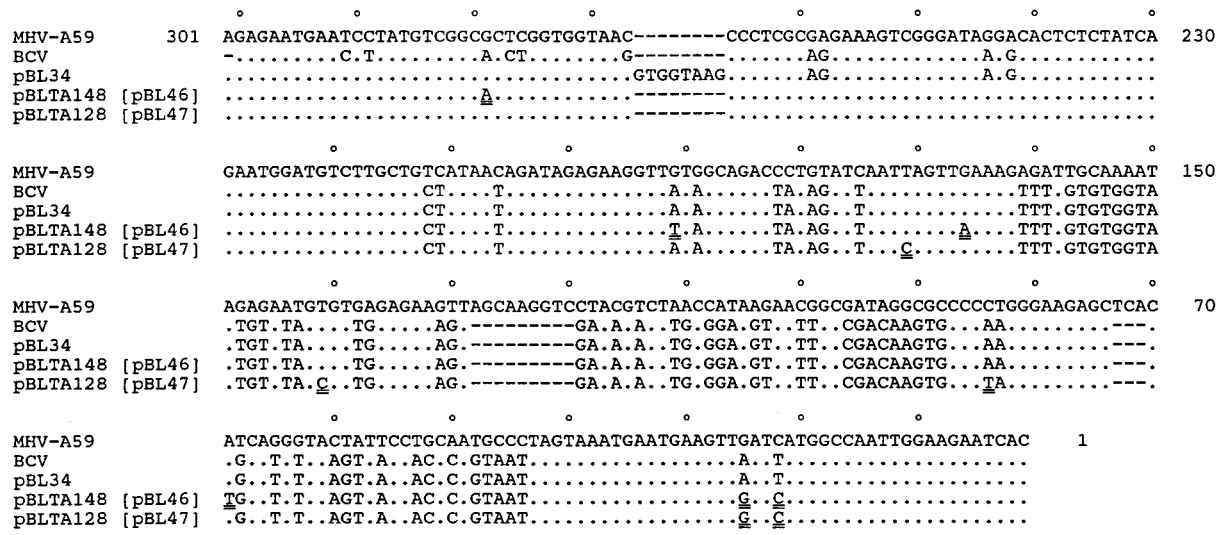

FIG. 4. Sequence alignment of the 3′ UTRs of MHV-A59 (GenBank accession no. M35256, with correction noted in reference 15) and BCV strain Mebus (GenBank accession no. M16620) shown as positive-strand DNA. Beneath these are shown the corresponding regions of pBL34 and the PCR clones pBLTA148 and pBLTA128 (and their DI vector derivatives pBL46 and pBL47, respectively). For the BCV and chimeric sequences, only the nucleotides that differ from MHV are given; dashes indicate gaps in the alignment. Mutated nucleotides in pBLTA148 and pBLTA128 are doubly underlined. Numbering is according to the MHV sequence, beginning at the nucleotide adjacent to the poly(A) tail and ending at the nucleotide following the N gene stop codon, with 10-nt intervals indicated by open circles above the alignment.

neous-size products of this first reaction was then further amplified by 30 cycles of the same PCR program with two primers, PM119 (nt 1077 to 1094 of the N gene) and PM112 (complementary to nt 18 to 35 of the MHV 3′ UTR). A single product of 566 bp was obtained, and it was purified and made blunt ended with T4 DNA polymerase. (The blunt terminus bounded by PM112 formed half of the *Msc*I site at the downstream end of the 3′ UTR.) The fragment was then restricted with *Bst*XI and exchanged for the *Bst*XI-*Msc*I fragment of pBL34. A plasmid pool, designated pMIX, was purified from approximately 21,000 combined colonies resulting from transformation of this ligation into *Escherichia coli* NM522.

RNA transcribed from pMIX was transfected into MHV-infected cells and found to harbor a subpopulation that was replication competent. Total cytoplasmic RNA extracted from these cells was reverse transcribed with a primer complementary to nt 1 to 18 of the 3′ UTR (these segments are identical in BCV and MHV) and then amplified by PCR with this primer and an upstream primer falling within the BCV N gene spacer B marker. The resulting PCR product was digested with *Sac*I to eliminate the background of MHV 3′ UTR-derived fragments, and the *Sac*I-resistant product was isolated and ligated into a TA cloning vector (pCRII; Invitrogen).

RESULTS

Inability to incorporate a 262-nt segment from the 3′ end of the BCV genome into the MHV genome. As an initial strategy for studying the *cis*-acting elements in the 3′ UTR of MHV that are essential for viral replication, we attempted to replace the 3′ UTR of MHV with that of BCV. Targeted RNA recombination was carried out to transduce the BCV 3′ UTR into the genome of Alb4, which is a thermolabile mutant of MHV A59 with an 87-nt deletion encompassing the N gene spacer B (15). In addition, Alb4 is temperature sensitive, forming tiny plaques at the nonpermissive temperature (39°C) that are clearly distinguishable from those formed by wild-type MHV.

The donor RNA carrying the BCV 3′ UTR was transcribed from a vector, pBL10 (Fig. 1A and Table 1), which was elsewhere identical to the N gene-containing MHV DI RNA vector pB36 that we had used previously in targeted RNA recombination (5, 24, 26, 27). In pBL10, a 262-nt segment corresponding the 3′ end of the BCV 3′ UTR (288 nt total) was abutted to the 5′ 35 nt of the MHV 3′ UTR (301 nt total) by use of available restriction enzyme sites. The junction formed was thus nonhomologous with respect to the alignment of the two sequences (Fig. 4), resulting in an 8-nt insertion (5′GTGGTAAG3′). We assumed that this insertion would be of no consequence, since a 5-nt insertion at the same point is known to be tolerated in a recombinant virus, Alb46, that we had constructed previously (15).

RNA transcribed from pBL10 was transfected into Alb4-infected cells, and recombinant viruses were selected as those able to form large plaques at 39°C. In four independent experiments, cytoplasmic RNA isolated from cells infected with 12 individual candidate recombinants was analyzed by sequencing. As expected, all recombinants contained the wild-type MHV N gene spacer B, which had repaired the Alb4 deletion. Surprisingly, however, each also contained the MHV 3′ UTR, not the BCV 3′ UTR (data not shown). Presumably, these recombinants arose by double crossovers. These results suggested that recombinants containing the 262 nt of the BCV 3′ UTR, if any were produced, were not viable.

Effect of the partial BCV 3′ UTR on the selection of double-crossover events. To ensure that the 12 recombinants were derived from double crossovers and not, somehow, from wild-type MHV contamination, a vector, pBL34, was designed in which a portion of the MHV N gene spacer B of pBL10 was replaced with a portion of the BCV N gene spacer B (Fig. 1A). This substitution, hereafter referred to as the BCV spacer B marker, has been previously shown to be phenotypically silent in MHV (28) and would thus act as a tag with which to unambiguously label recombinants. Two independent progeny viruses, Alb116 and Alb117, were selected from targeted recombination between pBL34-derived RNA and the Alb4 genome. The direct sequencing of genomic RNA isolated from each of the purified recombinant viruses showed the presence of the entire MHV 3′ UTR as well as the BCV spacer B marker (data not shown). The downstream crossover site for each was found to be located between the 3′ UTR and the N gene spacer B, while the upstream crossover had to have occurred within the N gene 5′ to spacer B (Fig. 1B). Therefore, this confirmed that recombinants obtained from prior targeted recombination with pBL10 donor synthetic RNA arose from double crossovers.

However, these results also raised the possibility that most of the targeted RNA recombinants we had previously obtained (5, 15, 24, 27, 28) actually came from double, not single, crossovers, because of a hypothetical high-frequency crossover site somewhere between spacer B and the 5′ 35 nt of the 3′ UTR. If this were true, then it would not be possible to obtain chimeric 3′ UTR recombinants even if parts of the BCV 3′ UTR were functionally interchangeable with parts of the MHV 3′ UTR. To examine this possibility, a vector, pBL31, was designed in which most of the N gene and 3′ UTR of MHV-1 was substituted for the corresponding region of MHV-A59 (Fig. 2). This introduced multiple variant nucleotides throughout the N gene and at both ends of the 3′ UTR. Three independent progeny viruses, Alb114, Alb115, and Alb120, were selected from recombination of pBL31 RNA with Alb4 recipient virus. These were analyzed in detail by sequencing of RNA from infected cells, and one (Alb114) was confirmed by direct RNA sequencing of purified genome. The sequence of each recombinant was consistent with its having been generated by only a single crossover event that occurred between nt 846 and 954 of the MHV A59 N gene (Fig. 2). Although we cannot rule out the possibility that a second crossover occurred within the 87 nt of the 3′ UTR adjacent to the poly(A) tail, these results clearly showed that it was possible to incorporate a functionally interchangeable region (that of MHV-1) into the 3′ end of the MHV A59 genome. Taken together, the data from the pBL34 and pBL31 experiments led us to conclude that the presence of the 262-nt fragment of the BCV 3′ UTR must be lethal when the fragment is recombined into the MHV genome, thereby accounting for the selection of only double-crossover recombinant viruses.

Inability of the pBL34 MHV-BCV chimeric RNA to replicate. It next became of interest to examine the replicative ability of pBL34-derived RNA, since it had been previously established that the RNA transcribed from pB36, the parent vector of pBL34, is an authentic replicating DI RNA (24). To explore this, we metabolically labeled wild-type MHV-infected cells that were transfected with pBL34 RNA. As a positive control, pB36 DI RNA was transfected into MHV-infected cells, and as negative controls, the same infected cells were mock transfected or were transfected with RNA from pBL50, which contains the BCV 3′ UTR in an inverted orientation. As shown in Fig. 3, in the presence of helper virus, cells transfected with pBL34 chimeric RNA and pBL50 synthetic RNA did not synthesize an extra RNA species between MHV A59 RNA6 and RNA7 (lanes 2 and 3). In contrast, replication of pB36 DI RNA was clearly detected (lane 4). Excluding the poly(A) tail, the sizes of RNA6 and RNA7 are 2,446 and 1,745 nt, respectively; the sizes of nonpolyadenylated pBL34, pBL50, and pB36 RNAs are 2,176, 2,176, and 2,183 nt, respectively. The failure of pBL34 to replicate with MHV as helper virus suggested that its replacement of the MHV 3′ UTR with that of BCV could have damaged or lost one or more *cis*-acting elements essential for replication or else that the 3′ UTRs of the two viruses are highly species specific and cannot be interchanged. It was not surprising that pBL34 RNA, although nonreplicating, could give rise to recombinants, since we have previously obtained recombinants with other nonreplicating donor RNAs (15, 27). It is noteworthy, though, that double-crossover events apparently were not as rare as we would have expected on the basis of the frequency of single-crossover events.

Mutation of pBL34 chimeric RNA into a replicating entity. We next sought to generate a functional DI RNA from the nonreplicating pBL34 chimeric RNA. We approached this by applying the DNA shuffling method developed by Stemmer (37, 38) to introduce multiple random mutations into the 3′ end of pBL34 (Fig. 3B). This process yielded pMIX, a pool of plasmids in which thousands of mutagenized plasmids were mixed together. We speculated that some of the RNA species transcribed from pMIX might have been mutated into functional DI RNAs. Indeed, radiolabeling of MHV-infected, pMIX RNA-transfected cells led to detection of an extra RNA band between RNA6 and RNA7 in two independent replication experiments, one of which is shown in Fig. 3A, lane 6.

To identify the mutations in one or more of the replicating RNA species, we analyzed cloned reverse transcription-PCR products made from cytoplasmic RNA isolated from pMIX-transfected cells. To amplify these, we used a negative-sense primer complementary to nt 1 to 18 of the 3′ UTR coupled with a positive-sense primer identical to a portion of the BCV spacer B marker. For reasons that remain unclear, the vast majority of clones obtained with this primer pair turned out to be the result of mispriming on cellular mRNAs. However, two independent clones containing a portion of the BCV 3′ UTR, pBLTA128 and pBLTA148, were identified. A third clone was found to be identical to pBLTA128. For both pBLTA128 and pBLTA148, nt 1 to 212 of the 3′ UTR were of BCV origin, whereas the remainder of the 3′ UTR (nt 213 to 301) came from MHV (Fig. 4). (Here and elsewhere, the coordinate system used is that of the MHV 3′ UTR, numbered from the 3′ end of the genome.) Both clones also contained the BCV spacer B marker in the N gene. In addition, six point mutations in the 3′ UTR were found in pBLTA148: T22C, A25G, A69T, G166A, A191T, and G279A (Fig. 4). In pBLTA128, there were seven point mutations: T22C, A25G, A84T, T141C, and T171C in the 3′ UTR and C1261T and A1358G in the N gene. The first of the N gene mutations created a stop codon, resulting in the truncation of the carboxy-terminal 34 amino acids of the N protein. Thus, the RNA molecules from which pBLTA148 and pBLTA128 originated appeared to have obtained mutations from multiple sources. First, a crossover was required to create the recombination in the 3′ UTR somewhere between nt 212 and 242, and at least one additional crossover was required for acquisition of the BCV spacer B marker. Second, point mutations distributed in the BCV 3′ UTR segment most likely were generated by the DNA shuffling mutagenesis. Third, point mutations located in the MHV 3′ UTR segment and the N gene must have been generated during viral RNA synthesis or else during reverse transcription and PCR. It should be noted that the T22C and A25G mutations in each clone (which change BCV nucleotides back to their MHV counterparts) resulted from the process of DNA shuffling because of the use of MHV primer PM112 to amplify the primerless PCR product (Fig. 3B).

To test whether the inserts in pBLTA148 and pBLTA128 truly represented sequences of replicating DI RNAs, the region from spacer B through the 3′ UTR of each was used to replace the corresponding region of pBL34, producing vectors pBL46 and pBL47, respectively (Fig. 5A). In multiple independent metabolic labeling experiments, replication of pBL46- and pBL47-derived RNAs was detected in the presence of wild-type helper virus (Fig. 5B, lanes 3 and 4). It was observed that the replication efficiency of pBL47 was diminished compared with that of pBL46, but this was most likely due to the truncation of the N gene open reading frame in pBL47 (3, 13, 41). The ability of these two RNAs to replicate indicated that the 3′ 212 nt of the MHV 3′ UTR and the 3′ 200 nt of the BCV 3′ UTR (possibly with some critical point mutations) were functionally interchangeable.

To understand whether this portion of BCV sequence could also function within the MHV genome, we next aimed at in-

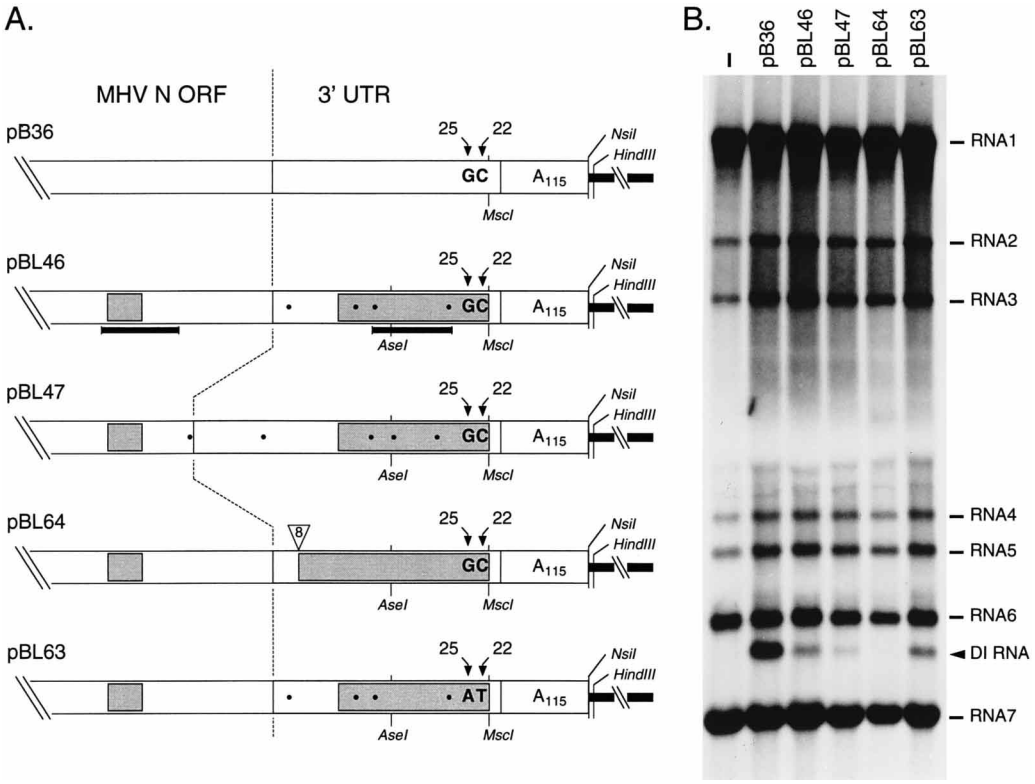

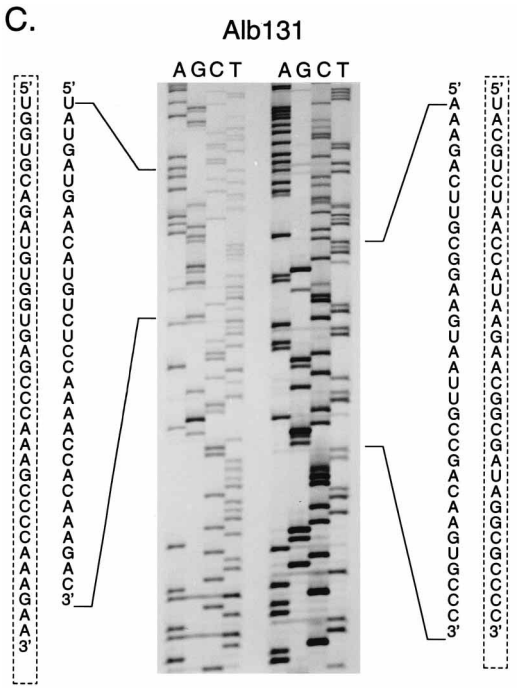

FIG. 5. Replicative ability of mutated DI RNAs derived from pBL34. (A) Construction of transcription vectors for the synthesis of MHV DI RNAs based on replicating RNAs selected from pMIX. Plasmids pBL46 and pBL47 were obtained by insertion of the cloned PCR products from pBLTA148 and pBLTA128, respectively, into a pBL34 background. Shaded rectangles indicate BCV sequence in portions of the 3′ UTR and the N gene spacer B; solid circles represent mutated nucleotides. In pBL47, the mutated nucleotide most upstream truncates the N gene open reading frame (ORF). Plasmid pBL64 is identical to pBL34 (Fig. 1), except that nt 22 and 25 of the 3′ UTR are mutated to C and G, respectively. Plasmid pBL63 is identical to pBL46, except that nt 22 and 25 of the 3′ UTR are mutated to T and A, respectively. (B) Wild-type MHV-infected cells were mock transfected (−) or transfected with the indicated DI RNA and then were labeled with 137 μCi of $^{32}P_i$ per ml. Purified cytoplasmic RNA was denatured with formaldehyde and formamide, separated by electrophoresis through 1% agarose containing formaldehyde (30), and visualized by autoradiography. (C) Portions of genomic RNA sequence from purified virions of recombinant Alb131 obtained with donor RNA from pBL46. The portions of the autoradiogram shown correspond to the lengths indicated by bars under pBL46 in panel A. The indicated segments of sequence shown within these, given as positive-sense RNA, represent the most divergent portions of the N gene spacer B (left) and the 3′ UTR (right); the corresponding MHV sequences (dotted line boxes) are shown for comparison.

corporating the 3′ UTRs of pBL46 and pBL47 into the MHV genome. A recombinant virus of wild-type phenotype, Alb131, was obtained after targeted recombination by use of pBL46 donor RNA with Alb4 as the recipient. Genomic RNA sequencing verified that it contained the BCV spacer B marker and the entire MHV-BCV chimeric 3′ UTR sequence identical to that of pBL46 (Fig. 5C). This demonstrated that the MHV replication machinery is able to recognize *cis*-acting elements embedded in the background of the sequence of this region of the BCV 3′ UTR, perhaps in conjunction with certain nucleotide changes. We were unable to obtain any recombinant viruses by using pBL47 as donor RNA. This was not unexpected, because although the truncation of the N open reading frame did not abolish the replicative ability of pBL47 DI RNA, it almost certainly was lethal to an essential structural gene in the context of the whole virus. These results indicated that the sequences contained in pBLTA148 and pBLTA128 did indeed represent portions of replication-competent DI RNA species that had been obtained through mutagenesis of the nonreplicating pBL34. In retrospect, it is not clear why we never obtained replicating DI RNAs with pBL34 by recombination with the MHV 3′ UTR between nt 212 and 242.

Analysis of the effect of nt 22 and 25 on replication. We next sought to determine what feature(s) possessed by pBL46 RNA enabled it to replicate, in contrast to RNA from its nonreplicating progenitor, pBL34. The two most salient differences between the two were (i) the homologous crossover from the BCV to MHV 3′ UTR upstream of nt 212 in pBL46, compared with the nonhomologous BCV-MHV junction at nt 266 in pBL34; and (ii) the MHV nucleotides at positions 22 and 25, which were inserted into pBL46, compared with the BCV nucleotides at these positions in pBL34 (Fig. 4). A third difference between the two was the set of four additional, apparently random point mutations in the 3′ UTR of pBL46. However, because of the lack of any concordance between these and the three additional 3′ UTR point mutations in pBL47 (Fig. 4), we assumed (correctly, as it turned out) that these had no significant effect on the replication competence of the DI RNAs.

We therefore initially focused attention on the nt 22 and 25 changes, since these fell in a region of the 3′ UTR (nt 1 to 55) that has been shown to contain a signal sufficient for MHV negative-strand RNA synthesis (19). To examine these, nt 22 and 25 in pBL34 were changed into the MHV residues C and G, respectively, yielding pBL64 (Fig. 5A). Conversely, the BCV residues T and A, respectively, were substituted for the same positions in pBL46 to give rise to pBL63 (Fig. 5A). These 2 nt changes in pBL34 and pBL46 RNAs did not have any effect on the replication status of these species (Fig. 5B): the nonreplicating pBL34 chimeric RNA did not become a functional DI RNA via the changes introduced into pBL64, nor did the pBL46 DI RNA lose its replication competence after alteration to pBL63. Thus, our results showed that the critical difference between pBL34 and pBL46 did not reside in the identity of residues 22 and 25 of the 3′ UTR.

A functionally essential bulged stem-loop RNA structure in the 3′ UTR. The segment of the 3′ UTR upstream of nt 212, which exhibits 10 nt differences between MHV and BCV, thus became of interest. To explore the possibility of a functionally significant RNA structure occurring in this region, we used the Mfold program of the Genetics Computer Group sequence analysis package (6). This analysis, in conjunction with our prior data, suggested a stem-loop structure, interrupted by five bulges, extending from nt 234 to 301 of the MHV 3′ UTR (Fig. 6). This region is absolutely conserved in all other MHV strains for which sequence is available, except for a substitution, in some cases, of G279A at one of the single-base bulge positions. Most significantly, the same secondary structure is predicted for the homologous segment of the BCV 3′ UTR, and this is the only structure in the entire 3′ UTR predicted by the Mfold program that is conserved between BCV and MHV. Eight of the 10 nt that differ between MHV and BCV in this region form four covariant base pairs in the stem portions of the structure: nt 242-nt 291, 244-nt 289, 258-nt 277, and 259-nt 276. In each case, an A-U base pair is changed to a G-C base pair, or vice-versa (Fig. 6). The remaining 2 nt that differ between MHV and BCV fall in the loop (nt 267) or in the same single-base bulge that varies in some of the MHV sequences (nt 279). Additional support for the proposed structure comes from two other coronaviruses in the same antigenic group, human coronavirus OC43 (HCV OC43 [11]) and bovine enteric coronavirus (BECV [2]; GenBank accession no. M36656), which have the same eight covariant stem nucleotides and the same nt 279 variant as BCV. HCV OC43 also exhibits two additional covariant base pairs, nt 249-nt 284, changing G-U to A-U, and nt 257-nt 278, changing G-C to A-U. BECV has one additional covariant base pair, nt 253-nt 280, changing G-C to G-U, and a different variant base in the loop, U270C.

Taken together, these considerations provided compelling

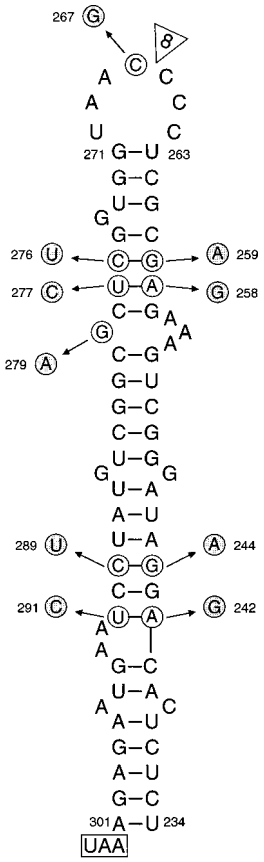

FIG. 6. Proposed RNA secondary structure immediately following the N gene stop codon (boxed). Numbering is according to the MHV sequence, as in Fig. 4. BCV nucleotides that differ from those of MHV are shown in shaded circles. The triangle indicates the point of the 8-nt insertion caused by the nonhomologous junction in pBL34 and in plasmids and RNAs derived therefrom.

phylogenetic evidence that the computer-generated structure was of actual functional significance. Moreover, the structure provided two potential explanations for the failure of pBL34 RNA to replicate. First, if the sequence composition of the loop were important, then the 8-nt insertion in pBL34 may have been deleterious (Fig. 4 and 6). Second, the composition of pBL34 chimeric RNA would have damaged the stem structure by attempting to pair the MHV left stem arm (upstream of the loop) with the BCV right stem arm (downstream of the loop), thus disrupting the base pairs at nt 244-nt 289 and 259-nt 276 (Fig. 6). In pBL46 (and pBL47), the sequence comprising the bulged stem-loop was purely of MHV origin and did not contain the loop insert, so the putative functionality of the secondary structure should have been intact.

To test these possibilities, a series of six DI template constructs were derived from pBL34 in which all combinations of MHV or BCV left and right arms of the stem were paired (Fig. 7A). Two of these constructs also tested the effect of the presence of the 8-nt insert within a homogeneous MHV or BCV stem-loop. The replicative ability of RNAs transcribed from these templates was assayed in duplicate independent metabolic labeling experiments, one of which is shown in Fig. 7B. We observed that all RNAs containing left and right stem arms from the same source, whether BCV (pBL82 and pBL77) or MHV (pBL75, pBL72, and the control pB36), were able to replicate in the presence of MHV helper virus. In contrast,

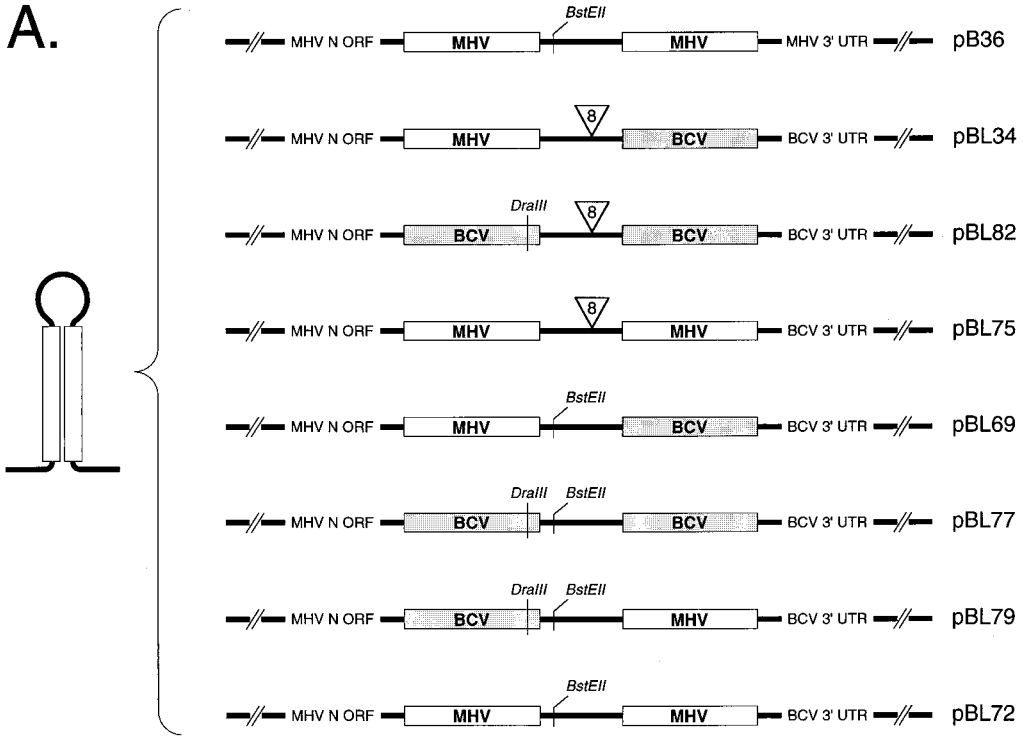

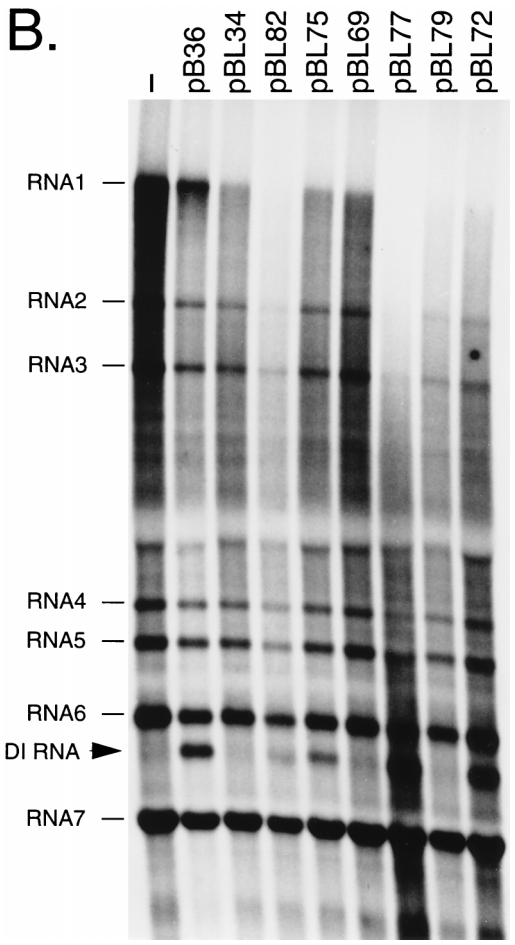

FIG. 7. Replicative ability of DI RNAs containing homogeneous or chimeric RNA secondary structures in the 3′ UTR. (A) Composition of plasmids containing different combinations of left and right arms of the putative bulged stem-loop structure, with or without the 8-nt insert (triangle) in the loop. Except for pB36, which is composed entirely of MHV components, all plasmids contain the authentic BCV 3′ UTR sequence downstream of the bulged stem-loop structure. ORF, open reading frame. (B) Wild-type MHV-infected cells were mock transfected (−) or transfected with the indicated DI RNA and then were labeled with 200 μCi of $^{32}P_i$ per ml. Purified cytoplasmic RNA was denatured with formaldehyde and formamide, separated by electrophoresis through 1% agarose containing formaldehyde (30), and visualized by autoradiography.

RNAs with mixed pairs of stem arms, whether BCV-MHV (pBL79) or MHV-BCV (pBL69 and the control pBL34), failed to replicate. This suggested that the bulged stem-loop structure is functionally essential for DI RNA replication and that its structure, rather than primary sequence, was of principal importance. In addition, the data showed that the presence of the 8-nt insertion in the loops of those DI RNAs harboring a homogeneous stem-loop did not abolish replicative ability (pBL82 and pBL75), although it may have attenuated replication somewhat compared with that of counterparts not containing the insertion (pBL77 and pBL72). The tolerance of this insertion is consistent with the viability of a 5-nt insertion in the same region, as shown previously (15).

To obtain corroborative support for the presence and functionality of the bulged stem-loop structure, we attempted to recombine each of the six synthetic RNAs into the MHV genome. Following transfection of these into Alb4-infected cells and selection by thermal inactivation, two independent recombinants were isolated from each donor RNA as progeny able to form wild-type-sized plaques at the nonpermissive temperature. After plaque purification, these were analyzed by sequencing of RNA from infected cells, which showed that independently obtained pairs were identical. For one member of each pair of successful recombinants, the viral RNA sequence was confirmed by direct sequencing of the entire 3′ UTR of purified genomic RNA, a portion of which is shown in

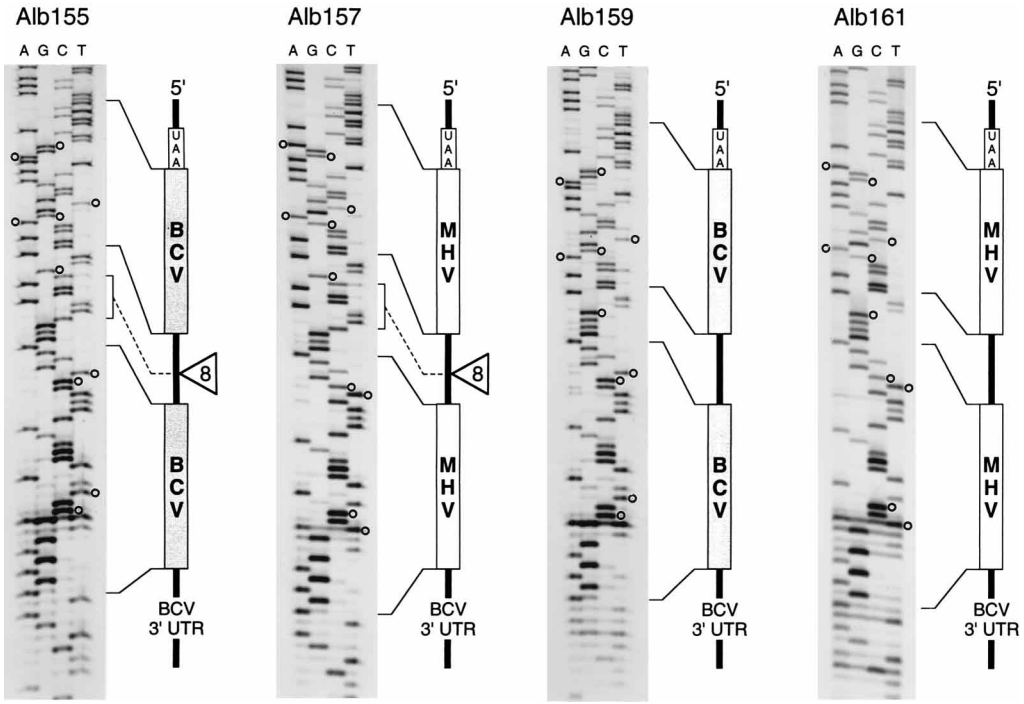

FIG. 8. Recombinant viruses obtained with donor DI RNAs with homogeneous left and right arms of the putative bulged stem-loop structure. Shown are portions of genomic RNA sequences of purified virions of recombinants Alb155, Alb157, Alb159, and Alb161 obtained, respectively, from the pBL82, pBL75, pBL77, and pBL72 donor DI RNAs. The left and right arms of the bulged stems, the loop, and the 8-nt insert are represented as in Fig. 7A. Open circles mark nucleotides that vary between the MHV and BCV 3′ UTRs.

Fig. 8. It was found that DI RNAs that contained homogeneous stem arms of either MHV or BCV origin (pBL82, pBL75, pBL77, and pBL72) could be recombined completely, from the N gene spacer B marker through the entire 3′ UTR, into the MHV genome. These gave rise, apparently via a single crossover event, to recombinants Alb155, Alb157, Alb159, and Alb161, respectively (Fig. 8). Although we have not examined the growth properties of these recombinant viruses in detail, they do not differ noticeably with respect to wild-type MHV. In contrast, the recombinants obtained with pBL69 and pBL79 RNAs contained the MHV 3′ UTR, not the chimeric 3′ UTR from each donor RNA. Like the recombinant viruses derived from pBL34 chimeric RNA, these were found to harbor the BCV N gene spacer B marker, which presumably was acquired through a double crossover. Thus, there was complete congruence between the ability of a given 3′ UTR to support DI replication and its ability to function within the intact viral genome. In summary, these data strongly indicate (i) the putative bulged stem-loop structure at the 5′ end of the 3′ UTR does indeed exist, and it is essential for MHV replication; (ii) the pairing, but not the primary sequence, of the four covariant base pairs is critical for the function of the structure; and (iii) the 8-nt insertion in the loop is tolerated by the virus.

DISCUSSION

Two principal conclusions can be drawn from the work presented here. First, it is possible to replace the 3′ UTR of MHV with that of BCV. Second, the 3′ UTR of each of these viruses contains a 68-nt bulged stem-loop structure immediately downstream of the N gene stop codon that at least in MHV, is essential for replication. Most critically, these results were not only demonstrated in constructed DI RNAs, but they were validated in the context of the intact viral genome.

In the replicating DI RNAs shown in Fig. 5B and 7B and in the recombinant MHV mutants shown in Fig. 5C and 8, large segments of the BCV 3′ UTR were exchanged for the homologous regions of the MHV 3′ UTR. In the most extreme case, that of DI RNA pBL77 and recombinant virus Alb159, the entire BCV 3′ UTR, with the exception of nt 267 (in the loop of the bulged stem-loop structure), replaced the entire MHV 3′ UTR. All recombinant viruses having chimeric BCV-MHV 3′ UTRs showed no obvious phenotypic differences from wild-type MHV, indicating either that regions of primary sequence variation between the two viruses perform in an identical manner or that they are dispensable for viral replication. Analysis of the aligned 3′ UTRs of MHV and BCV reveals an overall sequence divergence of 31%, but in the most divergent region, between nt 44 and 161, this jumps to 60% (Fig. 4). Curiously, within these limits, there is situated an octanucleotide motif of unknown significance, 5′GGAAGAGC3′ (nt 74 to 81), that is highly conserved among all coronavirus 3′ UTRs. Currently, our work cannot provide any information about why the two very divergent BCV and MHV segments are functionally equivalent. One potential explanation is that except for the conserved motif, this sequence is a nonessential portion of the MHV genome. Another possibility is that the sequence of this region is unimportant, but it serves to maintain a critical spacing between essential *cis*-acting elements in the 3′ UTR.

Within the more highly conserved portions of the BCV and MHV 3′ UTRs, there are previously identified elements of demonstrated functional importance. Lin et al. (19) have shown that all information necessary and sufficient for MHV negative-strand RNA synthesis resides in the 3′-terminal 46 to 55 nt of the 3′ UTR, in conjunction with some undetermined length of poly(A) tail. The corresponding BCV sequence varies only at its 5′ extreme (Fig. 4) plus at nt 22 and 25, the substi-

tution of which we have specifically shown to be inconsequential (Fig. 5). Contained within the signal for negative-strand RNA synthesis is an 11-nt motif, 5′UGAAUGAAGUU3′ (nt 26 to 36), shown by Yu and Leibowitz to be bound by a set of host proteins that may be involved in viral RNA synthesis (45, 46). These motifs are identical between BCV and MHV. However, a proposed second binding site for the same set of proteins further upstream, 5′UGAGAGAAGUU3′ (nt 129 to 139) (20a, 46), is poorly conserved at the corresponding position in the BCV sequence, nor is there any similarity in predicted secondary structure in this region. Hence, the consensus motif for the binding of these proteins may be more complex than originally supposed, or the second site may not exist in the BCV 3′ UTR or may be spaced differently. Very recently, it has also been shown that DI RNA replication is abolished by small deletions within the region of nt 129 to 154, which overlaps the second 11-nt motif (20a). Again, it is presently difficult to correlate this finding with our results, since the corresponding BCV sequence diverges by more than 50% (Fig. 4). However, there may well be sequence or structural relationships that are as yet inapparent between the functionally equivalent MHV and BCV 3′ UTRs.

We have presented evidence for an essential RNA secondary structure at the 5′ end of the MHV 3′ UTR, which was discovered through our initial unsuccessful efforts to substitute a nonhomologously spliced segment of the BCV 3′ UTR in place of its MHV counterpart. This yielded a chimeric RNA, pBL34 RNA, that was unable to replicate and could not be recombined into the MHV genome (Fig. 1 and 3). From pBL34 RNA, a replication- and recombination-competent derivative, pBL46 RNA, was selected (Fig. 3 to 5). Analysis of the fundamental difference between these two species pointed to a potential bulged stem-loop structure formed by nt 234 to 301 of the MHV 3′ UTR. The identical structure could be found in the BCV 3′ UTR, conserved through the covariance of the nucleotides in four of the base pairs of the stem (Fig. 6). In pBL34, which had been constructed by inadvertently splitting this structure within the loop, two of the covariant base pairs would have been disrupted by attempting to pair the MHV left arm of the stem with the BCV right arm of the stem. Strong support for the bulged stem-loop structure came from analysis of all combinations of left arm-right arm pairings. We found that RNAs that preserved a BCV-BCV or MHV-MHV stem pairing were replication-competent and could be recombined into the MHV genome (Fig. 7 and 8). Conversely, RNAs that mixed a BCV stem arm with an MHV stem arm could not replicate and could not replace the 3′ UTR in the MHV genome. Consistent with this result, it was determined that DI replication was not abolished by an 8-nt insertion in the loop of the secondary structure, and viruses would tolerate this insertion, provided it occurred within a homogeneous MHV or BCV bulged stem-loop. The lowest free energy structures predicted for mutants Alb155 and Alb157, containing the 8-nt insertion, as well as for the previously constructed Alb46 (15), containing a 5-nt insertion, each have a different loop and stem segment adjacent to the loop, in comparison with the structure shown in Fig. 6. This may indicate that the exact composition of the loop and of the immediately adjacent stem segment is not critical for the function of this structure. Alternatively, protein binding may induce the folding of the stem segment adjacent to the loop to be identical to that of the wild-type structure.

The essential nature of the bulged stem-loop may provide an explanation for the loss of replicative ability of some DI deletion mutants studied by others. The DIssE-derived mutants MR19 and MR20 constructed by Kim et al. (12) and the DIssF-derived mutant 0-1ΔNS of Lin and Lai (18) each had one endpoint within the bulged stem-loop, and so this may account for their failure to replicate. However, the deletions in all of these mutants were sufficiently large (144, 177, and 188 nt, respectively) that the possibility that other important elements within them were also truncated cannot be ruled out. A more fine-structure deletion analysis of the 3′ UTR remains to be done to more precisely delineate the required sequences or structures.

Preliminary evidence for an essential RNA pseudoknot in the 3′ UTR of BCV has been presented by Williams et al. (44). This structure, which would encompass nt 185 to 238 (in the coordinate system of Fig. 4), is conserved in MHV and presumably plays an analogous role in this virus. The upstream stem of the pseudoknot thus overlaps the most downstream 5 nt of the bulged stem-loop structure. Two explanations may account for this overlap. First, the base segment of our stem-loop (nt 234 to 241 and 292 to 301), as depicted in Fig. 6, may not actually be part of the structure. Second, the nucleotides in the overlap region may participate in both structures, which could exist in dynamic equilibrium at different steps of RNA replication, as may be the case for a stem-loop and pseudoknot in the 3′ UTR of poliovirus (10). Further analysis of both structures will be necessary to sort out these possibilities.

Functionally relevant RNA secondary structures are contained in the 3′ UTRs of many positive-sense RNA viruses. These include the tRNA-like structures found at the 3′ termini of numerous plant viruses (7, 43) and pseudoknots and stem-loops reported for picornaviruses (10, 39) and flaviviruses (35), all of which are thought to play roles in viral RNA synthesis. At present, we can only speculate about the function of the bulged stem-loop structure that we have found in the MHV 3′ UTR. Since it is well removed from the region that suffices for negative-strand RNA synthesis (19), we conclude that its essential role in replication must be in positive-strand RNA synthesis. Very recently, Lin et al. (20) found that in a DI RNA reporter construct, subgenomic RNA synthesis was abolished by the substitution of BCV sequence in the region that we are describing as the left arm of the 3′ UTR bulged stem-loop. This would imply that this structure is crucial for all MHV positive-strand RNA synthesis, genomic as well as subgenomic. Folding of the negative strand of nt 234 to 301 does not yield a potential structure that is conserved between MHV and BCV. This indicates, somewhat paradoxically, that the bulged stem-loop close to the 3′ end of positive-strand RNA governs positive-strand RNA synthesis. If the template for positive-strand RNA synthesis is double-stranded RNA (19), not single-stranded, negative-sense RNA, then this would seem to preclude a role for the bulged stem-loop in the initiation of positive-strand RNA synthesis via an interaction between the 5′ and 3′ portions of the template. However, two other roles, not mutually exclusive, can be envisioned for the bulged stem-loop. It may function in the termination and polyadenylation of nascent positive-strand RNA. Also, it may be required to maintain separation of the strands of the double-stranded template after they are unwound by helicase(s) on the leading edge of the viral RNA polymerase complex.

More-detailed mutagenesis, coupled with protein binding studies, will help to clarify the role played by the bulged stem-loop in MHV replication. Further work must be done to establish the exact structure and sequence constraints on individual stem segments and bulge and loop nucleotides. Our present understanding, drawn from the four covariant base pairs, is that base pairing, but not primary sequence, is critical, but this notion may be modified upon more extensive analysis. We would also like to know whether the structure participates

in larger RNA-RNA associations or whether it is specifically bound by host or viral proteins, although as yet, no viral or host protein binding site has been mapped to this region.

ACKNOWLEDGMENTS

We are grateful to Matthew Shudt and Tim Moran of the Molecular Genetics Core Facility of the Wadsworth Center for the synthesis of oligonucleotides. We thank Ding Peng for valuable suggestions made during the course of this work, and we are grateful to Savithra Senanayake and David Brian (University of Tennessee) for generously providing the BCV clone pLN.

This work was supported in part by Public Health Service grants AI 31622 and AI 39544 from the National Institutes of Health.

REFERENCES

1. **Chang, R.-Y., M. A. Hofmann, P. B. Sethna, and D. A. Brian.** 1994. *cis*-acting function for the coronavirus leader in defective interfering RNA replication. J. Virol. **68:**8223–8231.
2. **Cruciere, C., and J. Laporte.** 1988. Sequence and analysis of bovine enteritic coronavirus (F15) genome. I. Sequence of the gene coding for the nucleocapsid protein: analysis of the predicted protein. Ann. Inst. Pasteur Virol. **139:**123–138.
3. **De Groot, R. J., R. G. van der Most, and W. J. M. Spaan.** 1992. The fitness of defective interfering murine coronavirus DI-a and its derivatives is decreased by nonsense and frameshift mutations. J. Virol. **66:**5898–5905.
4. **Fichot, O., and M. Girard.** 1990. An improved method for sequencing of RNA templates. Nucleic Acids Res. **18:**6162.
5. **Fischer, F., D. Peng, S. T. Hingley, S. R. Weiss, and P. S. Masters.** 1997. The internal open reading frame within the nucleocapsid gene of mouse hepatitis virus encodes a structural protein that is not essential for viral replication. J. Virol. **71:**996–1003.
6. **Genetics Computer Group.** 1996. Program manual for the Wisconsin package. Version 9.0. Genetics Computer Group, Madison, Wis.
7. **Haenni, A.-L., S. Joshi, and F. Chapeville.** 1982. tRNA-like structures in the genomes of RNA viruses. Prog. Nucleic Acid Res. Mol. Biol. **27:**85–104.
8. **Hofmann, M. A., and D. A. Brian.** 1991. The 5′ end of coronavirus minus-strand RNAs contains a short poly(U) tract. J. Virol. **65:**6331–6333.
9. **Hofmann, M. A., S. D. Senanayake, and D. A. Brian.** 1993. A translation-attenuating intraleader open reading frame is selected on coronavirus mRNAs during persistent infection. Proc. Natl. Acad. Sci. USA **90:**11733–11737.
10. **Jacobson, S. J., D. A. M. Konings, and P. Sarnow.** 1993. Biochemical and genetic evidence for a pseudoknot structure at the 3′ terminus of the poliovirus RNA genome and its role in viral RNA amplification. J. Virol. **67:**2961–2971.
11. **Kamahora, T., L. H. Soe, and M. M. C. Lai.** 1989. Sequence analysis of nucleocapsid gene and leader RNA of human coronavirus OC43. Virus Res. **12:**1–9.
12. **Kim, Y.-N., Y. S. Jeong, and S. Makino.** 1993. Analysis of *cis*-acting sequences essential for coronavirus defective interfering RNA replication. Virology **197:**53–63.
13. **Kim, Y.-N., M. M. C. Lai, and S. Makino.** 1993. Generation and selection of coronavirus defective interfering RNA with large open reading frame by RNA recombination and possible editing. Virology **194:**244–253.
14. **Kingsman, S. M., and C. E. Samuel.** 1980. Mechanism of interferon action. Interferon-mediated inhibition of simian virus-40 early RNA accumulation. Virology **101:**458–465.
15. **Koetzner, C. A., M. M. Parker, C. S. Ricard, L. S. Sturman, and P. S. Masters.** 1992. Repair and mutagenesis of the genome of a deletion mutant of the coronavirus mouse hepatitis virus by targeted RNA recombination. J. Virol. **66:**1841–1848.
16. **Lai, M. M. C.** 1990. Coronavirus: organization, replication and expression of genome. Annu. Rev. Microbiol. **44:**303–333.
17. **Lai, M. M. C.** 1992. RNA recombination in animal and plant viruses. Microbiol. Rev. **56:**61–79.
18. **Lin, Y.-J., and M. M. C. Lai.** 1993. Deletion mapping of a mouse hepatitis virus defective interfering RNA reveals the requirement of an internal and discontiguous sequence for replication. J. Virol. **67:**6110–6118.
19. **Lin, Y.-J., C.-L. Liao, and M. M. C. Lai.** 1994. Identification of the *cis*-acting signal for minus-strand RNA synthesis of a murine coronavirus: implications for the role of minus-strand RNA in RNA replication and transcription. J. Virol. **68:**8131–8140.
20. **Lin, Y.-J., X. Zhang, R.-C. Wu, and M. M. C. Lai.** 1996. The 3′ untranslated region of coronavirus RNA is required for subgenomic mRNA transcription from a defective interfering RNA. J. Virol. **70:**7236–7240.

20a. **Liu, Q., W. Yu, and J. L. Leibowitz.** 1997. A specific host cellular protein binding element near the 3′ end of mouse hepatitis virus genomic RNA. Virology **232:**74–85.

21. **Luytjes, W., H. Gerritsma, and W. J. M. Spaan.** 1996. Replication of synthetic interfering RNAs derived from coronavirus mouse hepatitis virus-A59. Virology **216:**174–183.
22. **Makino, S., N. Fujioka, and K. Fujiwara.** 1985. Structure of the intracellular defective viral RNAs of defective interfering particles of mouse hepatitis virus. J. Virol. **54:**329–336.
23. **Makino, S., C.-K. Shieh, J. G. Keck, and M. M. C. Lai.** 1988. Defective interfering particles of murine coronavirus: mechanism of synthesis of defective viral RNAs. Virology **163:**104–111.
24. **Masters, P. S., C. A. Koetzner, C. A. Kerr, and Y. Heo.** 1994. Optimization of targeted RNA recombination and mapping of a novel nucleocapsid gene mutation in the coronavirus mouse hepatitis virus. J. Virol. **68:**328–337.
25. **Méndez, A., C. Smerdou, A. Izeta, F. Gebauer, and L. Enjuanes.** 1996. Molecular characterization of transmissible gastroenteritis coronavirus defective interfering genomes: packaging and heterogeneity. Virology **217:**495–507.
26. **Parker, M. M., and P. S. Masters.** 1990. Sequence comparison of the N genes of five strains of the coronavirus mouse hepatitis virus suggests a three domain structure for the nucleocapsid protein. Virology **179:**463–468.
27. **Peng, D., C. A. Koetzner, and P. S. Masters.** 1995. Analysis of second-site revertants of a murine coronavirus nucleocapsid protein deletion mutant and construction of nucleocapsid protein mutants by targeted RNA recombination. J. Virol. **69:**3449–3457.
28. **Peng, D., C. A. Koetzner, T. McMahon, Y. Zhu, and P. S. Masters.** 1995. Construction of murine coronavirus mutants containing interspecies chimeric nucleocapsid proteins. J. Virol. **69:**5475–5484.
29. **Penzes, Z., K. Tibbles, K. Shaw, P. Britton, T. D. K. Brown, and D. Cavanagh.** 1994. Characterization of a replicating and packaged defective RNA of avian coronavirus infectious bronchitis virus. Virology **203:**286–293.
30. **Sambrook, J., E. F. Fritsch, and T. Maniatis.** 1989. Molecular cloning: a laboratory manual, 2nd ed. Cold Spring Harbor Laboratory Press, Cold Spring Harbor, N.Y.
31. **Sanger, F., S. Nicklen, and A. R. Coulson.** 1977. DNA sequencing with chain-terminating inhibitors. Proc. Natl. Acad. Sci. USA **74:**5463–5467.
32. **Sawicki, S. G., and D. L. Sawicki.** 1990. Coronavirus transcription: subgenomic mouse hepatitis virus replicative intermediates function in RNA synthesis. J. Virol. **64:**1050–1056.
33. **Sethna, P. B., M. A. Hofmann, and D. A. Brian.** 1991. Minus-strand copies of replicating coronavirus mRNAs contain antileaders. J. Virol. **65:**320–325.
34. **Sethna, P. B., S.-L. Hung, and D. A. Brian.** 1989. Coronavirus subgenomic minus-strand RNAs and the potential for mRNA replicons. Proc. Natl. Acad. Sci. USA **86:**5626–5630.
35. **Shi, P.-Y., M. A. Brinton, J. M. Veal, Y. Y. Zhong, and W. D. Wilson.** 1996. Evidence for the existence of a pseudoknot structure at the 3′ terminus of the flavivirus genomic RNA. Biochemistry **35:**4222–4230.
36. **Siddell, S. G.** 1995. The *Coronaviridae*: an introduction p. 1–10. *In* S. G. Siddell (ed.), The *Coronaviridae*. Plenum Press, New York, N.Y.
37. **Stemmer, W. P. C.** 1994. Rapid evolution of a protein *in vitro* by DNA shuffling. Nature **370:**389–391.
38. **Stemmer, W. P. C.** 1994. DNA shuffling by random fragmentation and reassembly: *in vitro* recombination for molecular evolution. Proc. Natl. Acad. Sci. USA **91:**10747–10751.
39. **Todd, S., and B. L. Semler.** 1996. Structure-infectivity analysis of the human rhinovirus genomic RNA 3′ non-coding region. Nucleic Acids Res. **24:**2133–2142.
40. **van der Most, R. G., P. J. Bredenbeek, and W. J. M. Spaan.** 1991. A domain at the 3′ end of the polymerase gene is essential for encapsidation of coronavirus defective interfering RNAs. J. Virol. **65:**3219–3226.
41. **van der Most, R. G., W. Luytjes, S. Rutjes, and W. J. M. Spaan.** 1995. Translation but not the encoded sequence is essential for the efficient propagation of defective interfering RNAs of the coronavirus mouse hepatitis virus. J. Virol. **69:**3744–3751.
42. **van der Most, R. G., and W. J. M. Spaan.** 1995. Coronavirus replication, transcription, and RNA recombination, p. 11–31. *In* S. G. Siddell (ed.), The *Coronaviridae*. Plenum Press, New York, N.Y.
43. **Weiner, A. M., and N. Maizels.** 1987. tRNA-like structures tag the 3′ ends of genomic RNA molecules for replication: implications for the origin of protein synthesis. Proc. Natl. Acad. Sci. USA **84:**7383–7387.
44. **Williams, G. D., R.-Y. Chang, and D. A. Brian.** 1995. Evidence for a pseudoknot in the 3′ untranslated region of the bovine coronavirus genome: corona and related viruses. Adv. Exp. Med. Biol. **380:**511–514.
45. **Yu, W., and J. L. Leibowitz.** 1995. Specific binding of host cellular proteins to multiple sites within the 3′ end of mouse hepatitis virus genomic RNA. J. Virol. **69:**2016–2023.
46. **Yu, W., and J. L. Leibowitz.** 1995. A conserved motif at the 3′ end of mouse hepatitis virus genomic RNA required for host protein binding and viral RNA replication. Virology **214:**128–138.